Supplementary Material

An Integrated Microfluidic Platform for Selective and Real-Time Detection of Thrombin Biomarkers using a Graphene FET

Niazul I. Khan[1], Mohammad Mousazadehkasin[2], Sujoy Ghosh[3], John G. Tsavalas[2,3], Edward Song[1,3]

[1]Department of Electrical and Computer Engineering, University of New Hampshire, Durham, United States

[2]Department of Chemistry, University of New Hampshire, Durham, United States

[3]Center for Advanced Materials and Manufacturing Innovation, University of New Hampshire, Durham, United States

1. Device Fabrication

1.1. Graphene transfer

To transfer graphene onto the substrate, the monolayer graphene on polymer film was immersed in deionized water slowly while the graphene film protected by the sacrificial layer was detached from the support polymer film and remained floating on the water. The floating sacrificial layer/graphene layer was then collected by the patterned gold electrode substrate which was then dried at room temperature for 30 minutes followed by annealing on hot plate at 150 °C for 1 hour. To remove the top sacrificial layer, the sample was then treated with acetone for 1 hour followed by dipping into ethanol for another 1 hour. Finally, the sample was dried with an air gun and thermally annealed in an oven at 300 °C in argon atmosphere for 2 hours.

1.2. Microfluidic channel fabrication

The microfluidic channel was fabricated with a PDMS block using the cast molding technique (Nguyen et al., 2018). For this, an SU-8 (MicroChem Corp.) master mold with the desired channel pattern (width: 600 μm, height: 100 μm) was formed on silicon wafer surface. The degassed mixture of PDMS prepolymer and curing agent (Sylgard 184) mixed at a weight ratio

of 10:1 was poured on the prepared master mold. Then the PDMS block was cured at 60 °C for 4 hours and then peeled off from the SU-8 mold.

2. GFET Devices Labels

Table S1: Summary of the labels for the 6 GFET devices in the microfluidic-integrated GFET device.

Device #	Source/Drain electrodes	Gate electrode
GFET- 1	2/3	1
GFET- 2	3/4	1
GFET- 3	4/5	1
GFET- 4	6/7	10
GFET- 5	7/8	10
GFET- 6	8/9	10

3. Aptamer Packing Density Estimation

The change of surface charge (ΔQ) can be expressed as (Xu et al., 2017a),

$$\Delta Q = C \times \Delta V_D \quad (1)$$

Where, ΔV_D is the shift in Dirac voltage, and C is the total gate capacitance, which can be expressed in by the following equation (Xu et al., 2017a):

$$\frac{1}{C} = \frac{1}{C_{G1}} + \frac{1}{C_{G2}} + \frac{1}{C_Q} \quad (2)$$

Where, C_{G1} and, C_{G2} are the geometrical capacitances formed due to the electrical double layer capacitances on different interfaces and denote the capacitance between the graphene and solution, and the capacitance between the gate electrode and solution, respectively. d_1 and d_2 represent the plate distances for C_{G1} and C_{G2}, respectively where $d_1 = d_2 = d =$ Debye length. C_Q which is related to the Fermi level shift, denotes the quantum capacitance of graphene associated with finite density of states due to Pauli principle (Fernández-Rossier et al., 2007).

From the model of parallel plate capacitors, we can write the following expressions for C_{G1} and C_{G2}.

$$C_{G1} = \frac{S_{graphene}\varepsilon_r\varepsilon_0}{d} \text{ and } C_{G2} = \frac{S_{gate}\varepsilon_r\varepsilon_0}{d}$$

where, $S_{graphene}$ is the contact area between the electrolyte and graphene monolayer, S_{gate} is the contact area between the electrolyte and gold gate electrode, ε_0 is the vacuum permittivity ($8.854 \times 10^{-12} F/m$) and ε_r is the relative dielectric constant of PBS solution (80). Estimated Debye length for a 0.01 × PBS buffer concentration, $d = 7.3\ nm$.

$S_{graphene}$ can be expressed as:

$$S_{graphene} = L_{gf} \times W_{mc}$$

where, L_{gf} is length of the graphene film which equals to 5 mm or 5000 µm and W_{mc} is the width of the microfluidic channel that equals to 600 µm. Therefore,

$S_{graphene} = 30{,}0000\ \mu m^2$.

Similarly, S_{gate} can be expressed as:

$S_{gate} = L_{gate} \times W_{mc}$

where, L_{gate} is the width of each gate electrode which equals to 100 µm and W_{mc} is the width of the microfluidic channel that equals to 600 µm. Therefore,

$S_{gate} = 100 \times 600 = 60{,}000\ \mu m^2$.

Therefore, the geometrical capacitance values can be calculated as:

$$C_{G1} = \frac{S_{graphene}\varepsilon_r\varepsilon_0}{d} = \frac{30{,}0000 \times 10^{-12} \times 80 \times 8.854 \times 10^{-12}}{7.3 \times 10^{-9}} = 2.911 \text{ nF}$$

$$C_{G2} = \frac{S_{gate}\varepsilon_r\varepsilon_0}{d} = \frac{60{,}000 \times 10^{-12} \times 80 \times 8.854 \times 10^{-12}}{7.3 \times 10^{-9}} = 5.822 \text{ nF}$$

The total geometrical capacitance (C_{TG}) can be calculated as the series combination of C_{G1} and C_{G2} and the value yields, $C_{TG} = 1.941\ nF$.

The quantum capacitance C_Q can be expressed as:

$$C_Q = C_q \times S_{graphene}$$

where C_q is the quantum capacitance per unit area and the value is ~ 2 μF/cm^2 (Xu et al., 2017a). Therefore, $C_Q = 0.6$ nF.

Now, the total gate capacitance, C can be calculated from Equation (2) as: C= 0.458 nF.

From Figure 3 (D), the attachment of 27-mer thrombin-binding aptamer leads to a Dirac voltage shift, ΔV_{Dirac}= 403.9 mV.

So, $\Delta Q = C \times \Delta V_D = 0.458 \times 10^{-9} \times 403.9 \times 10^{-3} = 1.85 \times 10^{-10}$ C.

If the probe density is n, ΔQ can be written as:

$$\Delta Q = 27neS_{graphene}$$

$$\Rightarrow n = \frac{\Delta Q}{27eS_{graphene}} = \frac{1.85 \times 10^{-10}}{27 \times 1.6 \times 10^{-19} \times 30000 \times 10^{-12}} = 1.427 \times 10^{15}/m^2 = 1.427 \times 10^{11}/cm^2.$$

Therefore, the aptamer probe density can be estimated to be $1.4274 \times 10^{11}/cm^2$. This is equivalent to 26.5 nm aptamer probe spacing which is comparable to other reported values in literature (Ping et al., 2016).

4. Control Experiments

To examine the inertness of the bare graphene to thrombin, a set of control experiments were performed by exposing bare graphene to thrombin solution of various concentrations. As shown in Figure S1(A) in the Supplementary Information, no significant shift in the Dirac voltage is observed indicating non-responsive behavior of the bare unmodified graphene to thrombin. We also performed another set of control experiments to examine the adsorption behavior of thrombin on GFET device modified with a different aptamer sequence. In this case, the graphene was modified with anti-lysozyme aptamers and were exposed to different concentrations of thrombin solutions. The anti-lysozyme aptamer sequences were: 5□–NH_2–$(CH_2)_6$– ATC AGG GCT AAA GAG TGC AGA GTT ACT TAG -3□ (Cox and Ellington, 2001). The measured transfer curves are presented in Figure S1(B) which shows that there is no significant shift in the Dirac voltage, indicating negligible non-specific adsorption of thrombin protein during the sample flow.

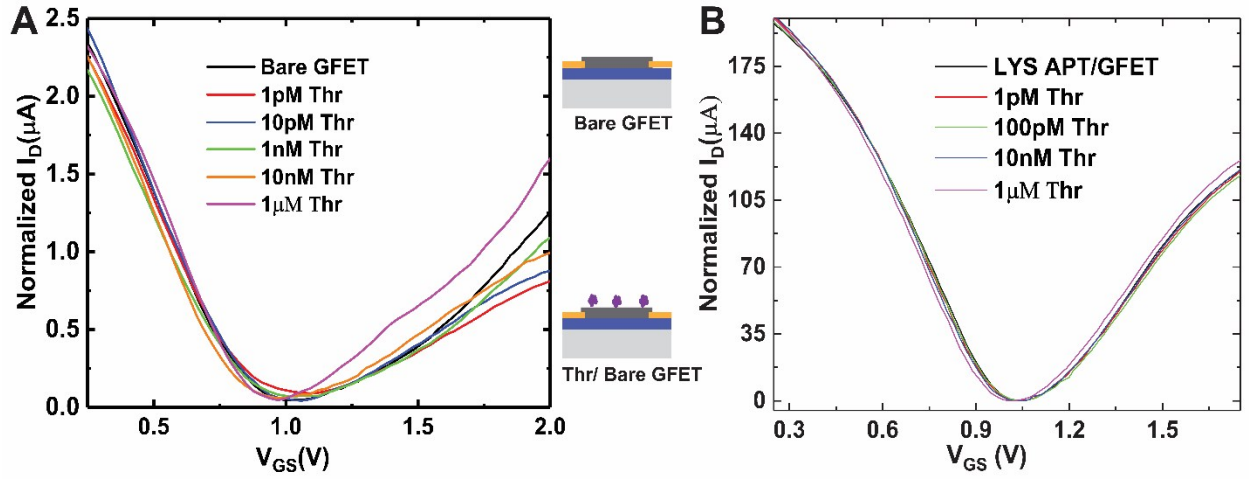

Figure S1: Control experiments. I_D-V_{GS} transfer curves of (A) bare graphene, and (B) lysozyme (LYS) aptamer modified graphene exposed to different concentrations (from 1 pM to 1 μM) of thrombin.

5. Calculation of Limit of Detection (LOD)

The limit of detection can be calculated according to the following equation:

$$LOD = \frac{3.3 \times standard\ deviation\ at\ the\ lowest\ concetration\ measured}{Slope\ of\ the\ calibration\ curve}$$

$$= \frac{3.3 \times 11.8521}{14.8715} = 2.63 \text{ pM}$$

6. Estimation of the half-life for PBASE dissociation from graphene surface

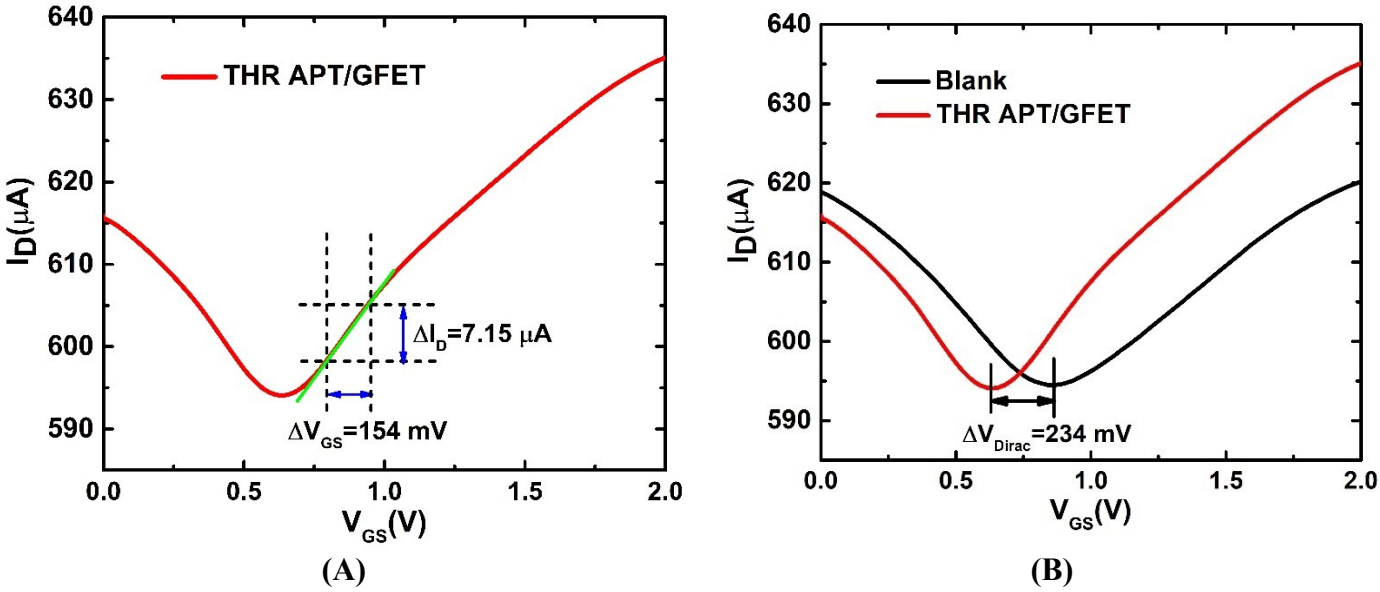

Figure S2. Calculation of the half-life for PBASE dissociation from graphene surface: (A) graphical illustration of finding transconductance g_m; and (B) Dirac voltage shift for aptamer immobilization on graphene surface.

From Fig S2(A), FET transconductance can be calculated by:

$$g_m = \frac{\Delta I_D}{\Delta V_{GS}} = 46.43 \text{ μS}$$

Now, the real-time measurements in Figure 5A, the baseline current shows an upward drift ($^{\Delta I_D}$) of 9.378 nA/min, which corresponds to a gate-source voltage shift, $^{\Delta V_{GS}} \approx 202$ μV/min.

The base-line current drift can be explained by the removal of aptamer from the graphene surface which is due to the graduate dissociation of pyrene anchor from the graphene surface. From Figure S2(B), we see that immobilization of aptamers cause a Dirac voltage shift ($^{\Delta V_{Dirac}}$) of 234 mV.

Therefore, half-life (λ) of PBASE dissociation can be found by calculating the time corresponding to $\frac{\Delta V_{Dirac}}{2} = 117$ mV. This can be found by:

$$\lambda = \frac{\Delta V_{Dirac}}{2 \times \Delta V_{GS}} = 579.21 \text{ min } \approx 10 \text{ hrs.}$$

7. Current Calibration Curve from Transient Measurements

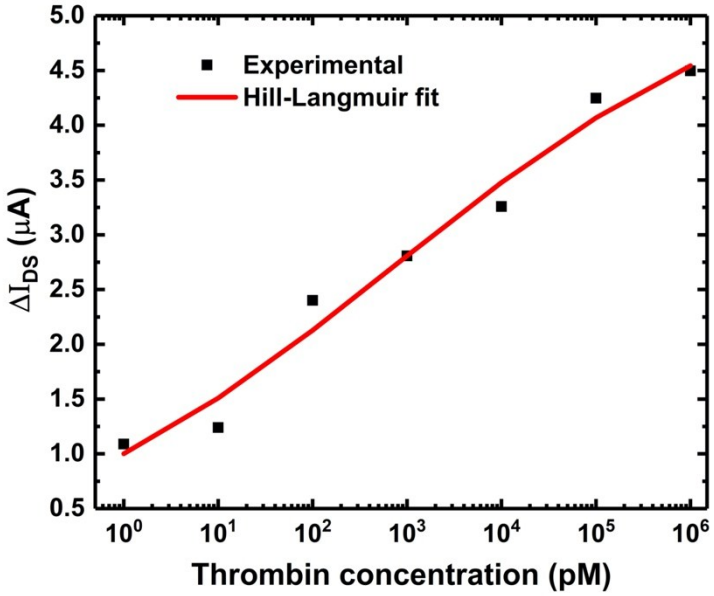

Figure S3. The concentration-dependent drain current (I_D) calibration plot and its Hill-Langmuir fit curve (R^2 = 97.78%).

The data can be fitted by the same Hill-Langmuir equation in the current domain:

$$\Delta I_D = \frac{I_0 + I_m\left(\frac{x}{K_D}\right)^n}{1 + \left(\frac{x}{K_D}\right)^n}$$

Table S2 summarizes the best fit (R^2=0.9778) values of the Hill-Langmuir equation. It gives a dissociation constant of K_D = 0.7317 nM which is comparable to the value obtained from the voltage calibration curve.

Table S2. Summary of the Hill Langmuir fitting parameters of the current calibration curve in Figure S3.

Hill-Langmuir parameters	Value	Error
I_0	-0.1729 μA	$\pm$ 2.6456 μA
I_m	5.6025 μA	$\pm$ 2.3776 μA
K_D	0.7317 nM	$\pm$ 1.8664 nM
n	0.2070	$\pm$ 0.2193

References

Fernández-Rossier, J., Palacios, J.J., Brey, L., 2007. Electronic structure of gated graphene and graphene ribbons. Phys. Rev. B 75, 205441.

Nguyen, N.V., Yang, C.H., Liu, C.J., Kuo, C.H., Wu, D.C., Jen, C.P., 2018. An Aptamer-Based Capacitive Sensing Platform for Specific Detection of Lung Carcinoma Cells in the Microfluidic Chip. Biosensors 8, 98.

Ping, J., Vishnubhotla, R., Vrudhula, A., Johnson, A.T.C., 2016. Scalable Production of High-Sensitivity, Label-Free DNA Biosensors Based on Back-Gated Graphene Field Effect Transistors. ACS Nano 10, 8700–8704.

Xu, S., Zhan, J., Man, B., Jiang, S., Yue, W., Gao, S., Guo, C., Liu, H., Li, Z., Wang, J., Zhou, Y., 2017. Real-time reliable determination of binding kinetics of DNA hybridization using a multi-channel graphene biosensor. Nat. Commun. 8, 14902.